Supporting information for

Inducing Preferential Growth of Zn (002) Plane by Multifunctional Chelator for Highly Reversible Zn Anode

Xi Li, [a] Zhenjie Chen, [a] Pengchao Ruan, [b] Xueting Hu, [b] Bingan Lu,[c] Xiaoming Yuan,[d]
Siyu Tian [b,e,*] and Jiang Zhou [b,*]

[a] Hunan Provincial Key Laboratory of Flexible Electronic Materials Genome Engineering, Changsha University of Science and Technology, Changsha 410004, China.

[b] School of Materials Science and Engineering, Hunan Provincial Key Laboratory of Electronic Packaging and Advanced Functional Materials, Central South University, Changsha 410083, China, E-mail: zhou_jiang@csu.edu.cn

[c] School of Physics and Electronics, Hunan University, Changsha 410082, China,

[d] Hunan Key Laboratory of Nanophotonics and Devices, School of Physics, Central South University, 932 South Lushan Road, Changsha 410083, China

[e] Department of Mechanical Engineering, The University of Texas at Dallas, 800 W Campbell Rd, Richardson, Texas 75080, United States. E-mail: siyu.tian@utdallas.edu

Experimental section

Materials: D-sodium gluconate ($C_6H_{11}NaO_7$, 99%), Ammonium metavanadate (NH_4VO_3, 99.95%), Zinc sulfate ($ZnSO_4 \cdot 7H_2O$, 99%) and N-methyl pyrrolidone (NMP, >99%) were purchased from Shanghai Aladdin Biochemical Technology Co., Ltd. Ethanedioic acid dihydrate ($H_2C_2O_4 \cdot 2H_2O$, ≥99.8%) was purchased from Sinopharm Chemical Reagent Co., Ltd. Super P (battery grade) and polyvinylidene fluoride (PVDF, battery grade) were purchased from Soochow DoDoChem Technology Co., Ltd.

Electrolyte preparation：$ZnSO_4 \cdot 7H_2O$ was dissolved into deionized (DI) water to prepare the 2 M $ZnSO_4$ (ZS) electrolyte. Different concentrations (10, 20, 50, 80, 100 mM) of sodium gluconate (SG) were added into the 2 M $ZnSO_4$ solutions (denoted as SG10, SG20, SG50 and SG80) to obtain the electrolytes for subsequent tests.

Preparation of $NH_4V_4O_{10}$ cathode materials: 2.106 g of NH_4VO_3 was dissolved in 90 mL of DI water and stirred at 80 °C until the solution became yellow. Then, 3.4038 g of $H_2C_2O_4 \cdot 2H_2O$ was added slowly and kept stirring to obtain a dark blue-green solution. The obtained solution was transferred to a 50 mL Teflon-lined autoclave and kept at 140 °C for 48 hours. The solid materials were collected and repeatedly washed with DI water and then dried at 80 °C overnight to obtain the $NH_4V_4O_{10}$ powers.

Material characterizations: X-ray diffraction (XRD) measurements were carried out on the Rigaku Mini Flex 600 diffractometer with Cu K α -radiation (λ =1.5418 Å). The surface morphology of Zn anodes was characterized by optical microscope (LW50LJT) and scanning electron microscope (SEM, MIRA3 TESCAN, 10 kV).

Electrochemical measurements: All CR2016-type coin cells using glass fiber separator were assembled in open-air environment. Galvanostatic charge-discharge (GCD) cycling tests were conducted at room temperature on NEWARE battery tester (CT-4008T-5V50mA-164) and LAND battery tester (LAND CT2001, China). Cyclic voltammetry (CV), chronoamperometry (CA) and

electrochemical impedance spectroscopy (EIS) tests were performed on electrochemical workstation (CHI660E, China). Linear sweep voltammetry (LSV) tests were performed at a scan rate of 5 mV s^{-1} in a three-electrode configuration, in which Ag/AgCl electrode was used as the reference electrode. In the LSV tests, all the electrolytes were based on 1 M Na_2SO_4 solutions.

Computational methods: Density functional theory (DFT) calculations were utilized to investigate the interactions of H_2O, SG, Zn^{2+} on different Zn crystal planes. The adsorption energies of them were calculated by the Vienna ab-initio simulation package (VASP). The generalized gradient approximation (GGA) with the Perdew-Burke-Ernzerhof (PBE) function was used as the exchange-correlation function. Firstly, we generated k-point meshes using VASPKIT with a 3×5×1 k-point mesh in the Monkhorst-Pack scheme, and the cutoff energy was set as 500 eV. Next, the convergence criteria of energy and force were set as 1×10^{-6} eV and 0.02 eV/atom, respectively. The Zn(002) surface had a 4×4 supercell in *ab* dimension. The absorption energies between Zn slab and various particles were defined as the following equation:

$$E_{aborb} = E_{tot} - E_{Zn-slab} - E_{molecules}$$

where E_{aborb}, E_{tot}, $E_{Zn-slab}$ and $E_{molecules}$ represent the adsorption energy, total energy of the system, energy of the Zn slab and energy of the isolated adsorbed molecules, respectively.

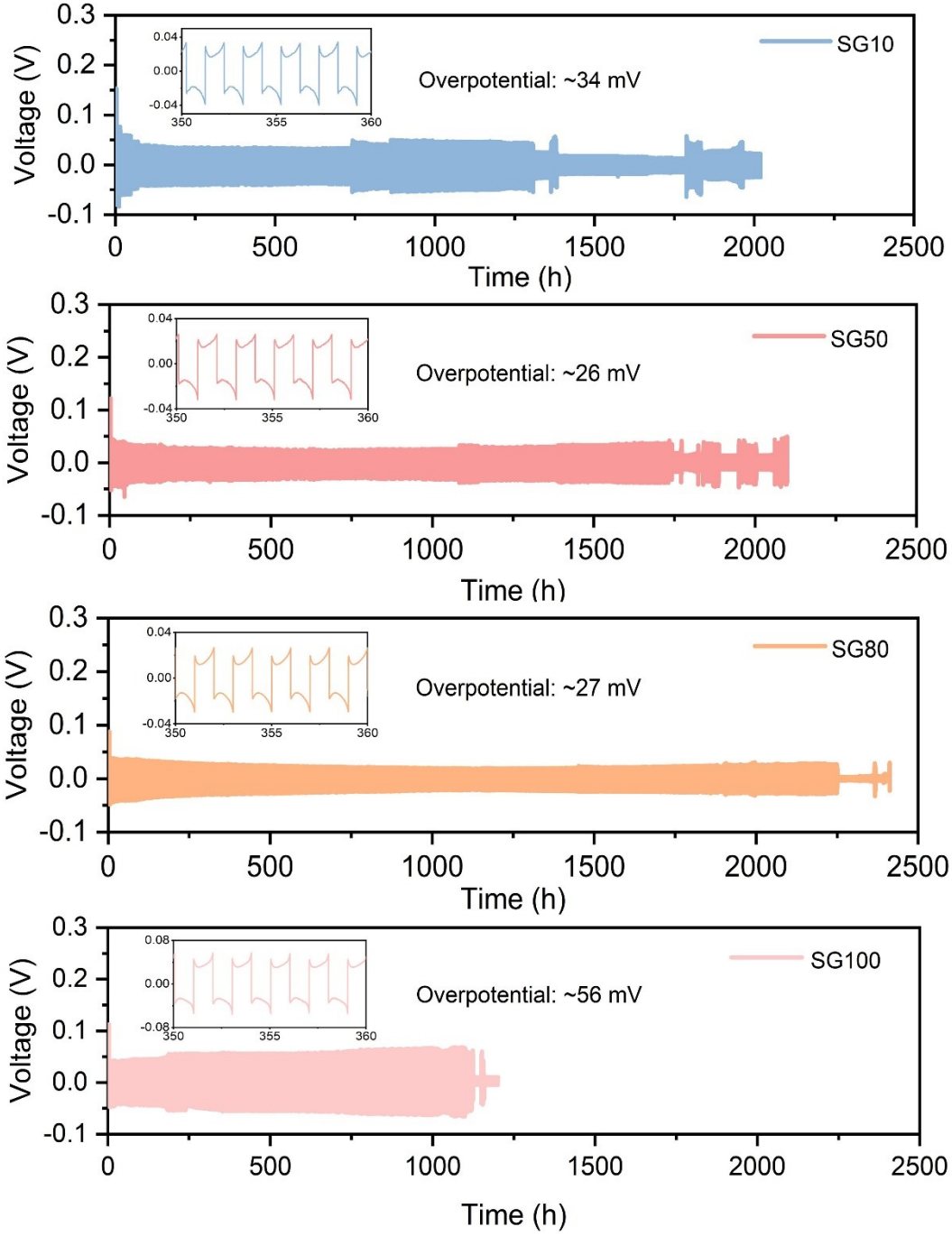

Fig. S1. Long-term cycling performance of Zn||Zn symmetric cells based on SG10, SG50, SG80 and SG100 electrolytes at 1 mA cm^{-2}, 1 mA h cm^{-2}.

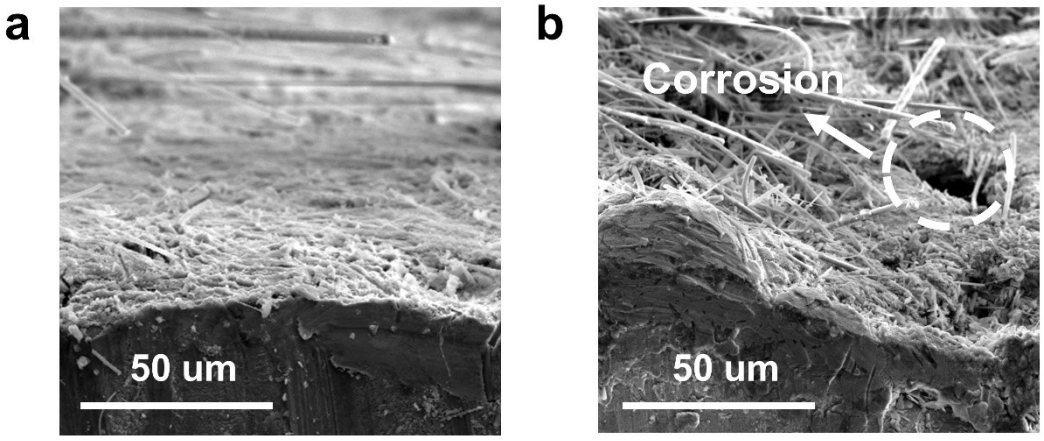

Fig. S2. Cross-sectional SEM images of the Zn anodes after 25 cycles at 5 mA cm^{-2}, 2.5 mA h cm^{-2} in (a) SG20 and (b) ZS electrolytes.

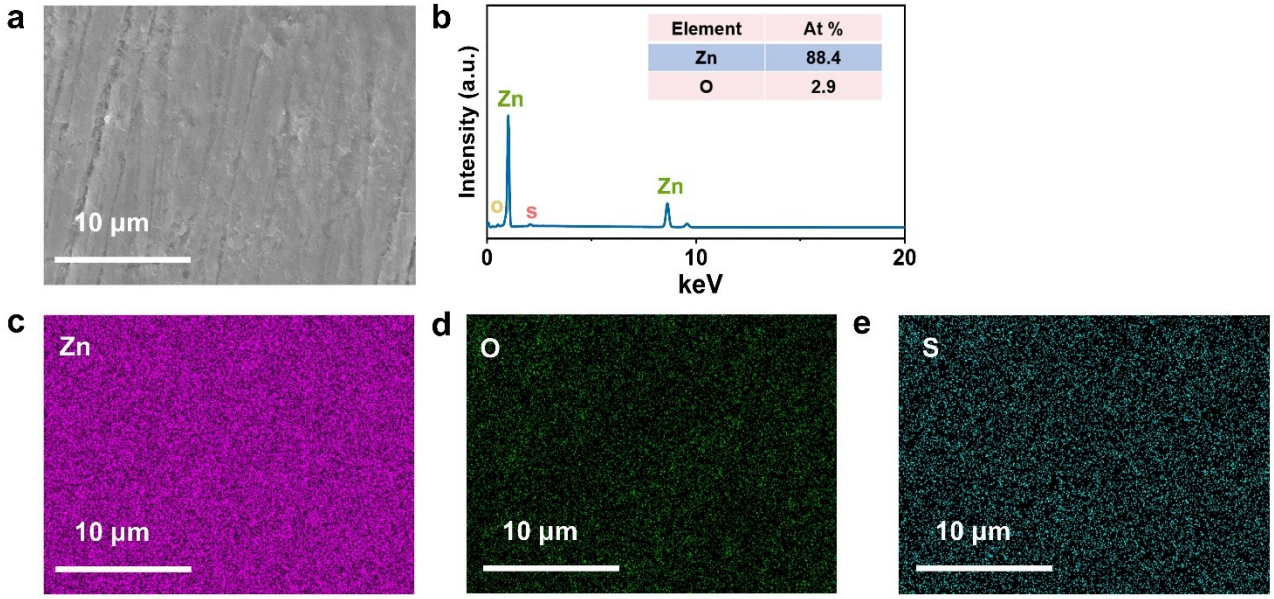

Fig. S3. EDS spectrum and elemental mappings of the Zn anode surface after cycling in SG20 electrolyte at 5 mA cm^{-2}, 2.5 mA h cm^{-2}.

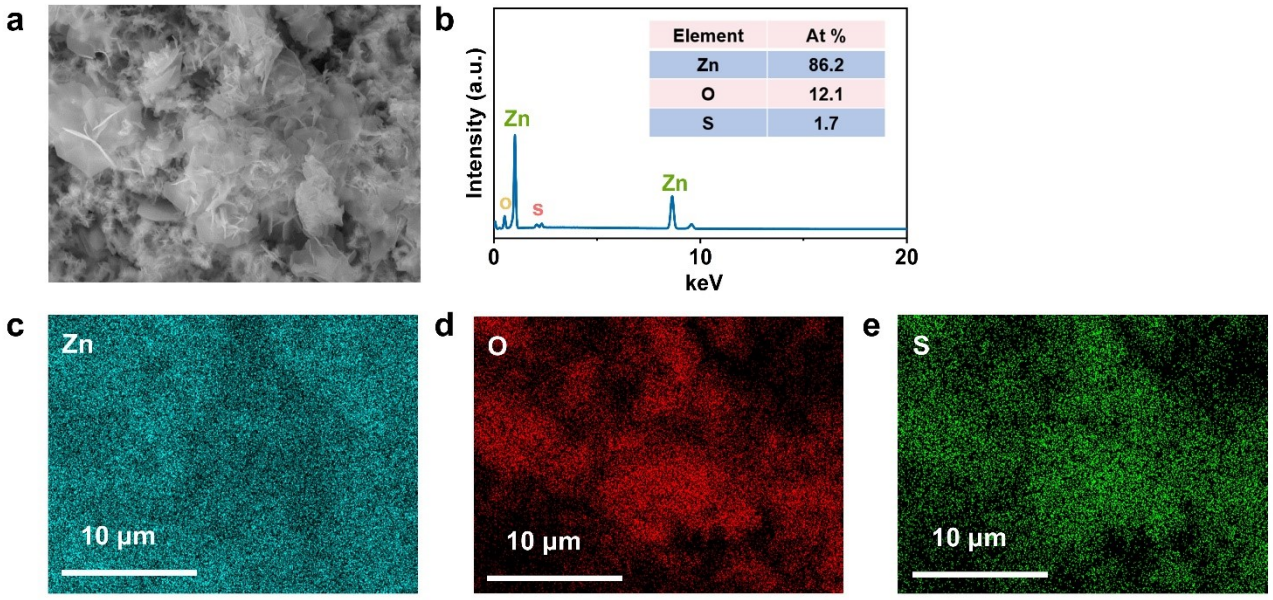

Fig. S4. EDS spectrum and elemental mappings of the Zn anode surface after cycling in ZS electrolyte at 5 mA cm^{-2}, 2.5 mA h cm^{-2}.

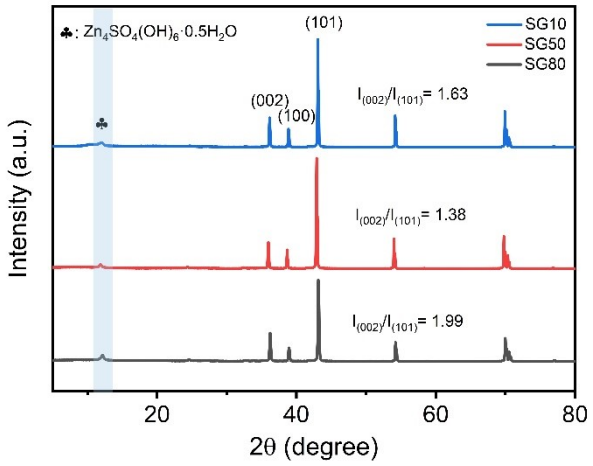

Fig. S5. XRD patterns of the Zn anodes in SG-based Zn||Zn symmetric cells after 50 cycles at 1 mA cm^{-2}, 1 mA h cm^{-2}.

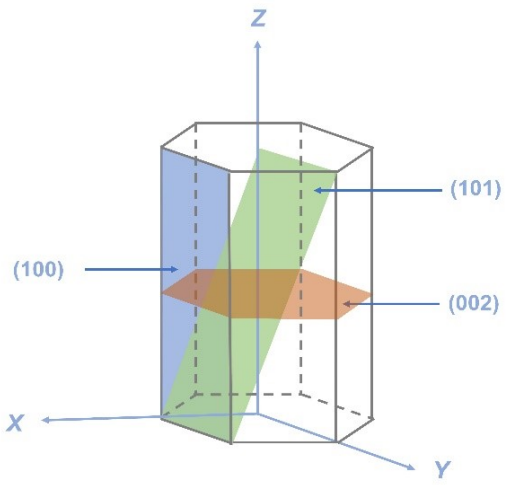

Fig. S6. The hexagonal close-packed structure of Zn.

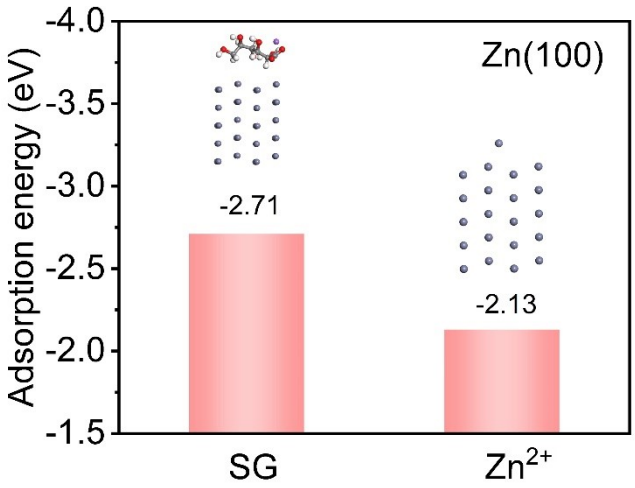

Fig. S7. Adsorption energies of SG and Zn^{2+} on the Zn (100) plane.

Fig. S8. Optical images of Zn soaked in SG20 and ZS electrolytes.

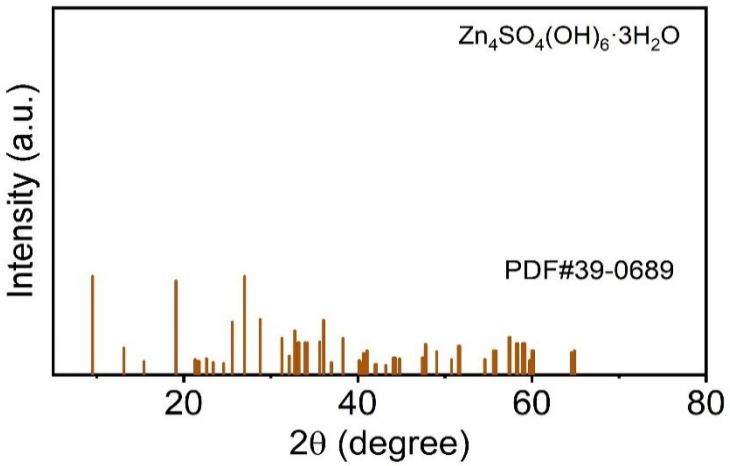

Fig. S9. Standard XRD pattern of $Zn_4SO_4(OH)_6·3H_2O$.

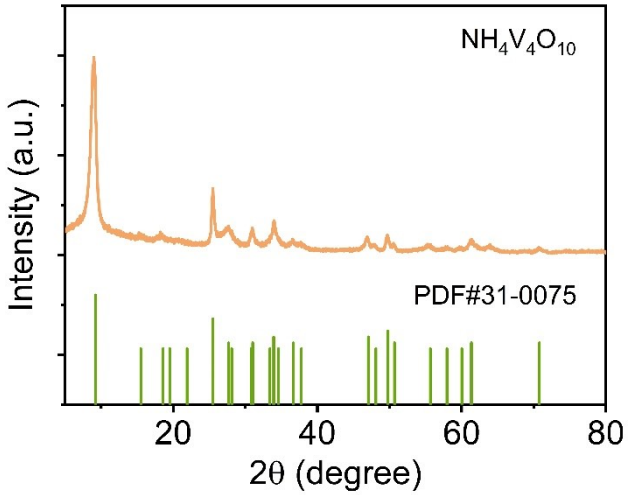

Fig. S10. XRD pattern of $NH_4V_4O_{10}$.

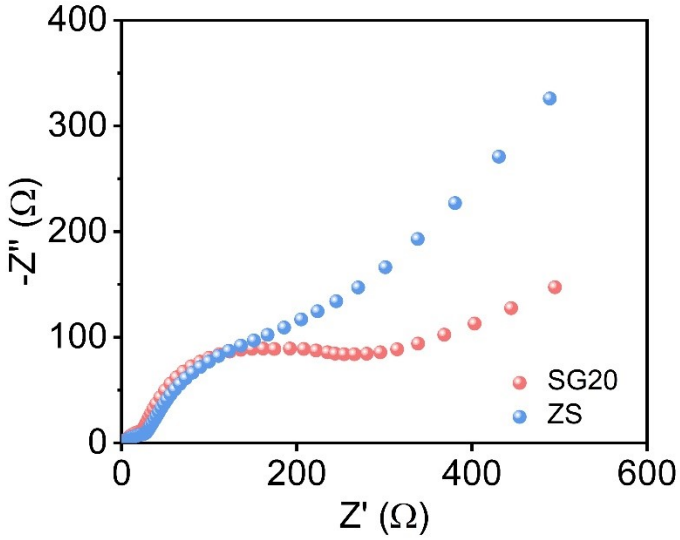

Fig. S11. EIS of Zn||$NH_4V_4O_{10}$ full cells based on SG20 and ZS electrolytes.

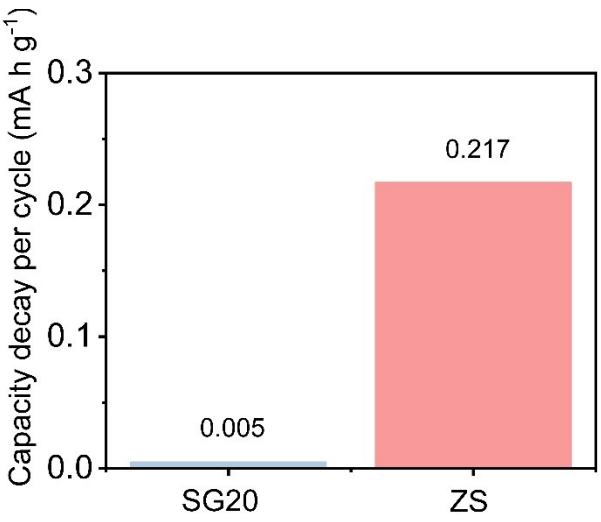

Fig. S12. Capacity decay rates of Zn||$NH_4V_4O_{10}$ full cells based on SG20 and ZS electrolytes at a current density of 5 A g^{-1}.

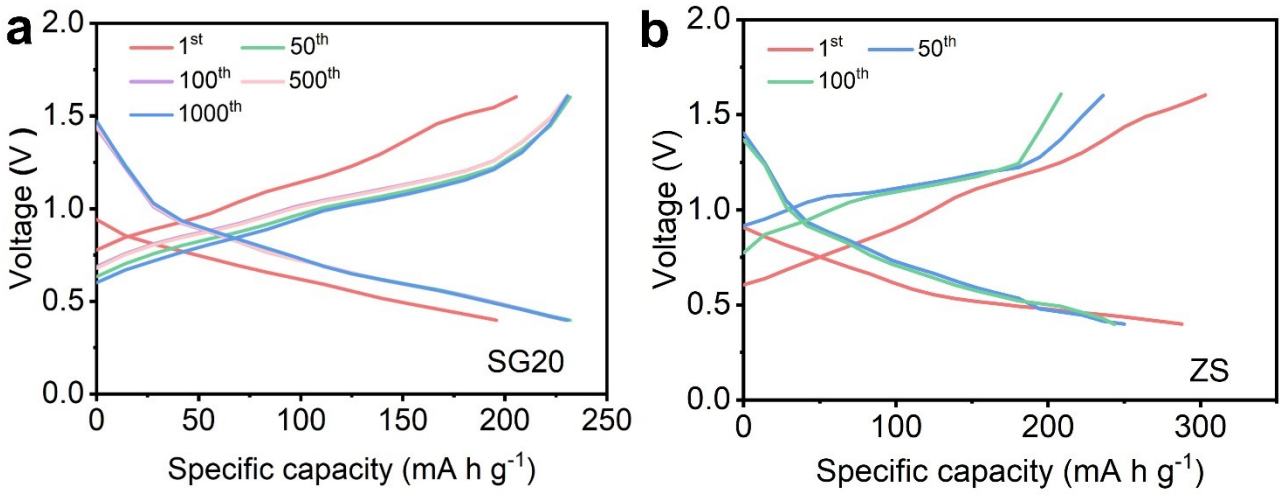

Fig. S13. Voltage profiles of Zn||$NH_4V_4O_{10}$ full cell based on (a) SG20 and (b) ZS electrolytes at a current density of 5 A g^{-1}.